Rational Design of Antimicrobial C3a Analogues with Enhanced Effects against Staphylococci Using an Integrated Structure and Function-Based Approach †

ARTICLE *in* BIOCHEMISTRY · OCTOBER 2008

Impact Factor: 3.02 · DOI: 10.1021/bi800991e · Source: PubMed

5 AUTHORS, INCLUDING:

Mukesh Pasupulti
Central Drug Research Institute
65 PUBLICATIONS **965** CITATIONS
SEE PROFILE

Björn Walse
SARomics
41 PUBLICATIONS **1,233** CITATIONS
SEE PROFILE

Artur Schmidtchen
Lund University
127 PUBLICATIONS **3,592** CITATIONS
SEE PROFILE

BIOCHEMISTRY
including biophysical chemistry & molecular biology

Article

Rational Design of Antimicrobial C3a Analogues with Enhanced Effects against Staphylococci Using an Integrated Structure and Function-Based Approach

Mukesh Pasupuleti, Bjo#rn Walse, Bo Svensson, Martin Malmsten, and Artur Schmidtchen

Biochemistry, **2008**, 47 (35), 9057-9070• DOI: 10.1021/bi800991e • Publication Date (Web): 09 August 2008

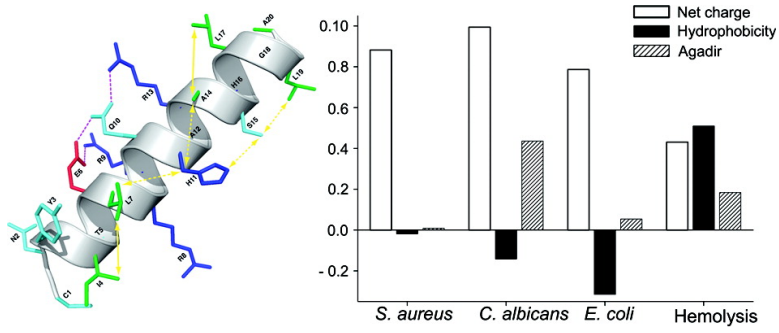

More About This Article

Additional resources and features associated with this article are available within the HTML version:

- Supporting Information
- Access to high resolution figures
- Links to articles and content related to this article
- Copyright permission to reproduce figures and/or text from this article

View the Full Text HTML

Articles

Rational Design of Antimicrobial C3a Analogues with Enhanced Effects against Staphylococci Using an Integrated Structure and Function-Based Approach†

Mukesh Pasupuleti,‡ Björn Walse,§ Bo Svensson,§ Martin Malmsten,|| and Artur Schmidtchen*,‡

Section of Dermatology and Venereology, Department of Clinical Sciences, Lund University, Biomedical Center, Tornavägen 10, SE-221 84 Lund, Sweden, SARomics AB, P.O. Box 724, SE-220 07 Lund, Sweden, and Department of Pharmacy, Uppsala University, SE-751 23 Uppsala, Sweden

Received February 15, 2008; Revised Manuscript Received July 2, 2008

ABSTRACT: The anaphylatoxin C3a and its inactivated derivative C3adesArg, generated during complement activation, exert direct antimicrobial effects, mediated via its C-terminal region [Nordahl et al. (2004) *Proc. Natl. Acad. Sci. U.S.A. 101*, 16879−16884]. During evolution, this region of C3a displays subtle changes in net charge, while preserving a moderate but variable amphipathicity [Pasupuleti et al. (2007) *J. Biol. Chem. 282*, 2520−2528]. In this study, we mimic these evolutionary changes, employing a design approach utilizing selected amino acid substitutions at strategic and structurally relevant positions in the original human C3a peptide CNYITELRRQHARASHLGLA, followed by structure−activity studies incorporating sequence-dependent QSAR models as tools for generation of C3a peptide variants with enhanced effects. While the native peptide and related amphipathic analogues of moderate positive net charge were active against the Gram-negative *Escherichia coli*, activity against the Gram-positive *Staphylococcus aureus* was primarily observed for peptides characterized by a combination of a relatively high net charge (+6−7) and a propensity to adopt an α-helical conformation with amphipathic character. Such increased helicity and charge also conferred activity against the fungus *Candida albicans*. A central histidine residue (H11), evolutionarily conserved among vertebrates, conferred high selectivity toward microbes, while substitutions with leucine rendered the peptides hemolytic. Selected C3a analogues retained their specificity against staphylococci in the presence of human plasma, while showing low cytotoxicity. The work illustrates structure−activity relationships underlying the function and specificity of antimicrobial C3a and related analogues and provides insights into the forces that drive evolution of antimicrobial peptides.

It has been estimated that humans contain about 1 kg of bacteria (~10^{14} cells) (*1*), an observation that reflects our coexistence with colonizing microbes. In order to control this microbial flora, humans as well as virtually all life forms are armored with a rapidly acting antimicrobial system based on short cationic and amphiphilic antimicrobial peptides (AMP).[1] Most AMPs are linear peptides, many of which may adopt an α-helical and amphipathic conformation upon bacterial binding (*2–8*). Amphipathic and α-helical AMPs, such as the human cathelicidin LL-37, magainin-2, PGLa, and pleurocidin, adopt highly ordered amphipathic helices in relevant phospholipid and ionic environments (*2–8*). However, the exact molecular mechanisms governing these processes, which have implications for AMP activities against Gram-negative and Gram-positive bacteria, as well as for toxicity against mammalian cells, are only just starting to be understood (*4, 7, 9–13*). Considering the increasing resistance problems against conventional antibiotics, AMPs have recently emerged as potential therapeutic candidates. Various strategies, such as use of combinational library approaches (*14*), stereoisomers composed of D-amino acids (*15*) or cyclic D,L-α-peptides (*16*), and high-throughput based screening assays (*17, 18*), are currently employed in the development of therapeutically interesting AMPs (*19, 20*).

We have previously shown that the human anaphylatoxin peptide C3a exerts a direct and potent antimicrobial effect against bacteria and fungi (*21, 22*). C3 deficiency is also connected with increased susceptibility to bacterial infections in humans (*23*), as well as in animal models (*24, 25*), findings

† This work was supported by grants from the Swedish Research Council (projects 13471 and 621-2003-4022), the Welander-Finsen, Crafoord, Söderberg, Schyberg, Alfred Österlund, and Kock Foundations, DermaGen AB, and The Swedish Government Funds for Clinical Research (ALF).

* Corresponding author. Tel: +46462224522. Fax: +4646157756. E-mail: artur.schmidtchen@med.lu.se.

‡ Department of Clinical Sciences, Lund University.

§ SARomics AB.

|| Department of Pharmacy, Uppsala University.

[1] Abbreviations: AMP, antimicrobial peptide; C3a, complement peptide 3a; CFU, colony-forming units; CF, carboxyfluorescein; QSAR, quantitative structure−activity relationship; PLS, partial least squares; RDA, radial diffusion assays; TSB, trypticase soy broth; TH, Todd−Hewitt; MH, Mueller−Hinton.

10.1021/bi800991e CCC: $40.75
Published on Web 08/09/2008

compatible with this direct antibacterial effect of C3a (*25*). The carboxy-terminal region of the anaphylatoxin peptide C3a is released by neutrophilic enzymes, harbors typical features of helical AMPs, and is protective against systemic infection with *Streptococcus pyogenes* (*22*). Previous studies also indicated that natural selection, affecting antimicrobial activity of this C3a region, favors changes in charge, while preserving a moderate amphipathicity. Thus, notwithstanding a significant sequence variation, functional and structural constraints imposed on C3a during evolution have preserved critical properties governing antimicrobial activity (*26*). During the course of these previous studies we noted that the human natural C3a peptide, being active against several Gram-negative bacteria *in vitro*, as well as against *S. pyogenes* also *in vivo*, displayed limited activity against the Gram-positive *Staphylococcus aureus*. Given this, the objectives of this study were 2-fold. First, we wanted to generate an understanding for the structural basis governing activity of this helical AMP against bacteria and fungi, as well as eukaryotic cells. Second, we wanted to identify C3a peptide analogues with enhanced activities against Gram-positive bacteria, such as *S. aureus*. Obviously, a design approach using systematic alterations of all possible positions in the amino acid framework of the peptide would not be feasible. For example, replacement of each position with only four amino acids would generate 4^{20} ($\sim 1 \times 10^{12}$) individual peptides. Here, we therefore adopted a strategy based on selected amino acid alterations in the peptide template, utilizing structural considerations, current knowledge on structural prerequisites for helix stabilization (*27, 28*), and bacterial as well as eukaryotic data, combined with peptide sequence dependent QSAR modeling for identification of novel C3a peptide variants with enhanced antimicrobial effects.

EXPERIMENTAL PROCEDURES

Peptides. Peptides were from Sigma-Genosys, generated by a peptide synthesis platform (PEPscreen, Custom Peptide Libraries, Sigma Genosys). Yield was ~1−6 mg, and peptide length 20 amino acids throughout. MALDI-ToF mass spectrometry was performed on these peptides, and average crude purity of the 20mers was found to be 60−70%. Peptides were supplied lyophilized and in a 96-well tube rack. Prior to biological testing the PEPscreen peptides were diluted in dH_2O (5 mM stock) and stored at −20 C. This stock solution was used for the subsequent experiments. Selected C3a variant peptides were synthesized by Innovagen AB, Lund, Sweden, and Sigma Genosys, U.K. The purity (>95%) and molecular weight of these peptides were confirmed by both suppliers by mass spectral analysis (MALDI.TOF Voyager). Biopeptide, San Diego, CA, synthesized the peptides Novisprin and Omiganan. Polymyxin B was from Sigma Genosys (purity >95%).

Microorganisms. Escherichia coli 37.4, *S. aureus* ATCC 29213, and *Candida albicans* ATCC 90028 were obtained from the Department of Clinical Bacteriology at Lund University Hospital. Additional *S. aureus* clinical isolates were obtained from patients with skin infections. *S. aureus* molecular typing was performed using ADSRRS-fingerprinting analysis (*29*). Briefly, *S. aureus* DNA was digested with the two restriction enzymes *Bam*HI (10 units/μL) (Sigma) and *Xba*I (10 units/μL) (Sigma). Cohesive ends of DNA were ligated with adapters and amplificated. PCR products were electrophoresed on polyacrylamide gels, stained by ethidium bromide, and photographed under UV light.

Radial Diffusion Assay. Essentially as described earlier (*22, 30*) bacteria were grown to midlogarithmic phase in 10 mL of full-strength (3% w/v) trypticase soy broth (TSB) (Becton-Dickinson, Cockeysville, MD). The microorganisms were then washed once with 10 mM Tris, pH 7.4. Subsequently, 4×10^6 bacterial colony-forming units was added to 15 mL of the underlay agarose gel, consisting of 0.03% (w/v) TSB, 1% (w/v) low electroendosmosis type (EEO) agarose (Sigma, St. Louis, MO), and 0.02% (v/v) Tween 20 (Sigma). The underlay was poured into a Ø 144 mm Petri dish. After agarose solidification, 4 mm diameter wells were punched, and 6 μL of test sample was added to each well. Plates were incubated at 37 C for 3 h to allow diffusion of the peptides. The underlay gel was then covered with 15 mL of molten overlay (6% TSB and 1% Low-EEO agarose in distilled H_2O). Antimicrobial activity of a peptide is visualized as a zone of clearing around each well after 18−24 h of incubation at 37 C.

Viable-Count Analysis. S. aureus ATCC 29213 bacteria were grown to midlogarithmic phase in Todd−Hewitt (TH) medium (Becton and Dickinson, Baltimore, MD). They were then washed and diluted in 10 mM Tris, pH 7.4, containing 5 mM glucose. Following this, bacteria (50 μL, 2×10^6 cfu/mL) were incubated, at 37 C for 2 h, with the peptides 100, 100H-L, 122, 122H-L, and LL-37 (at 0.03, 0.06, 0.3, 0.6, 3, 6, 30, 60 μM) in 10 mM Tris and 0.15 M NaCl with 20% human citrate−plasma. To quantify the bactericidal activity, serial dilutions of the incubation mixtures were plated on TH agar, followed by incubation at 37 C overnight, and the number of colony-forming units was determined. 100% survival was defined as total survival of bacteria in the same buffer and under the same condition in the absence of peptide. Significance was determined using the statistical software SigmaStat (SPSS Inc., Chicago, IL).

Hemolysis Assay. EDTA blood was centrifuged at 800*g* for 10 min, whereafter plasma and buffy coat were removed. The erythrocytes were washed three times and resuspended in 5% PBS, pH 7.4. The cells were then incubated with end-over-end rotation for 1 h at 37 C in the presence of peptides (60 μM). Triton X-100 (2%) (Sigma-Aldrich) served as positive control. The samples were then centrifuged at 800*g* for 10 min. The absorbance of hemoglobin release was measured at λ 540 nm and is in the plot expressed as % of Triton X-100 induced hemolysis.

Minimal Inhibitory Concentration Assay (MIC). MIC analysis, defining the lowest concentration of the AMP that prevents microbial growth, was carried out by a microtiter broth dilution method (*31*) with modifications to minimize interference by anionic compounds in the conventional growth medium, yielding less unspecific interactions and enhanced sensitivity (*32*). For preparation of polyanion-depleted (refined) media, 100 mL of Luria−Bertani broth was made in Tris, pH 7.4, and applied to a column packed with 40 mL of DEAE-Sephacel (Sigma, 9013-34-7). The column was previously rinsed with water, 2 M NaCl, 0.1 M NaOH, water, and 70% ethanol, respectively, and finally equilibrated 10 mM Tris, pH 7.4, before use. The medium was passed through the column twice and finally filter

sterilized (Millex GP filter unit 0.22 μm) and stored at 8 C until use. For determination of MIC, peptides were dissolved in 10 mM Tris, pH 7.4, at a concentration 5 times higher than the required range by serial dilutions from a stock solution. Twenty microliters of each concentration was added to each corresponding well of a 96-well microtiter plate (polypropylene; Costar Corp., Cambridge, MA). Bacteria grown overnight in 3% TSB were rinsed with Tris, pH 7.4, and diluted in refined LB medium to get a concentration of $\sim 1 \times 10^5$ CFU/mL. One-hundred microliters of bacterial solution in the refined LB medium was added to each well containing the test peptides. The plate was incubated at 37 C overnight. The MIC was taken as the concentration at which greater than 95% of growth inhibition was observed.

Flow Cytometry. S. aureus bacteria were grown to midlogarithmic phase in TH medium and washed in 0.15 M NaCl and 10 mM Tris, pH 7.4. The bacteria (2.5×10^7 cfu) were incubated for 2 h with LL-37 or the 100 and 100H-L peptides (30 μM) in 0.15 M NaCl and10 mM Tris with 20% human citrate−plasma in a total volume of 250 μL. The bacteria were then fixed by incubation on ice for 5 min and at room temperature for 45 min in 4% paraformaldehyde. Propidium iodide (Invitrogen) was added (9 μM), and the samples were incubated at room temperature for 15 min. Flow cytometry analysis was performed using a FACS-Calibur flow cytometry equipped with a 15 mW argon laser turned at 488 mm (Becton-Dickinson, Franklin Lakes, NJ). The bacterial population was selected by gating with appropriate settings of forward scatter (FSC) and sideward scatter (SSC). The FL2 fluorescence channel was used to record the emitted fluorescence of propidium iodide.

Lactate Dehydrogenase (LDH) Assay. HaCaT keratinocytes were grown in 96-well plates (3000 cells/well) in serum-free keratinocyte medium (SFM) supplemented with bovine pituitary extract and recombinant EGF (BPE-rEGF) (Invitrogen) to confluency. The medium was then removed, and 100 μL of the peptides investigated (at 60 μM, diluted in SFM/BPE-rEGF) was added in triplicate to different wells of the plate. The LDH-based TOX-7 kit (Sigma-Aldrich, St. Louis, MO) was used for quantification of LDH release from the cells. Results given represent mean values from triplicate measurements. Results are given as fractional LDH release compared to the positive control consisting of 1% Triton X-100 (yielding 100% LDH release).

MTT Assay. Sterile filtered MTT (3-(4,5-dimethylthiazolyl)-2,5-diphenyltetrazolium bromide; Sigma-Aldrich) solution (5 mg/mL in PBS) was stored protected from light at −20 C until usage. HaCaT keratinocytes, 3000 cells/well, were seeded in 96-well plates and grown in keratinocyte-SFM/BPE-rEGF medium to confluency. Peptides investigated were then added at 60 μM. After incubation overnight, 20 μL of the MTT solution was added to each well, and the plates were incubated for 1 h in CO_2 at 37 C. The MTT-containing medium was then removed by aspiration. The blue formazan product generated was dissolved by the addition of 100 μL of 100% DMSO per well. The plates were then gently swirled for 10 min at room temperature to dissolve the precipitate. The absorbance was monitored at 550 nm, and results given represent mean values from triplicate measurements.

Fluorescence Microscopy. For study of membrane permeabilization using the impermeant probe FITC, *S. aureus* ATCC 29213 bacteria were grown to midlogarithmic phase in TSB medium. The bacteria were washed and resuspended in either 10 mM Tris, pH 7.4, or 10 mM glucose to yield a suspension of 1×10^7 cfu/mL. The bacterial suspension (100 μL) was incubated with 30 μM of the respective peptides at 30 C for 30 min. Microorganisms were then immobilized on poly(L-lysine)-coated glass slides by incubation for 45 min at 30 C, followed by addition onto the slides of 200 μL of FITC (6 μg/mL) in the appropriate buffers and incubated for 30 min at 30 C. The slides were washed, and bacteria were fixed by incubation, first on ice for 15 min and then at room temperature for 45 min in 4% paraformaldehyde. The glass slides were subsequently mounted on slides using Prolong Gold antifade reagent mounting medium (Invitrogen). For fluorescence analysis, bacteria were visualized using a Nikon Eclipse TE300 (Nikon, Melville, NY) inverted fluorescence microscope equipped with a Hamamatsu C4742-95 cooled CCD camera (Hamamatsu, Bridgewater, ME) and a Plan Apochromat 100× objective (Olympus, Orangeburg, NY). Differential interference contrast (Nomarski) imaging was used for visualization of the microbes themselves.

Liposome Preparation and Leakage Assay. The liposomes investigated were either zwitterionic (DOPC/cholesterol, 60/40 mol/mol) or anionic (DOPC/DOPA/cholesterol, 30/30/40 mol/mol). DOPA (1,2-dioleoyl-*sn*-glycero-3-phosphate, monosodium salt) and DOPC (1,2-dioleoyl-*sn*-glycero-3-phoshocholine) were both from Avanti Polar Lipids (Alabaster, AL) and of >99% purity, while cholesterol (>99% purity) was from Sigma-Aldrich (St. Louis, MO). The latter was added for reducing spontaneous liposome leakage to less than a couple of percent over the time scale of the experiment. Due to the long, symmetric and unsaturated acyl chains of these phospholipids, several methodological advantages are reached. In particular, membrane cohesion is good, which facilitates very stable, unilamellar, and largely defect-free liposomes (observed from cryo-TEM) and well-defined supported lipid bilayers (observed by ellipsometry and AFM), allowing very detailed values on leakage and adsorption density to be obtained. Although seemingly somewhat suboptimal as a bacterial membrane model, it has previously been shown that semiquantitatively similar effects of peptide modifications such as length, charge, hydrophobicity, and topology are obtained for zwitterionic and anionic phospholipid membranes (*33, 34*), as well as from such liposomes with or without cholesterol present (*33–35*). The lipid mixtures were dissolved in chloroform, whereafter the solvent was removed by evaporation under vacuum overnight. Subsequently, 10 mM Tris buffer, pH 7.4, was added together with 0.1 M carboxyfluorescein (CF) (Sigma, St. Louis, MO). After hydration, the lipid mixture was subjected to eight freeze−thaw cycles consisting of freezing in liquid nitrogen and heating to 60 C. Unilamellar liposomes, of about Ø 140 nm were generated by multiple extrusions through polycarbonate filters (pore size 100 nm) mounted in a LipoFast miniextruder (Avestin, Ottawa, Canada) at 22 C. Untrapped carboxyfluorescein (CF) was then removed by two subsequent gel filtrations (Sephadex G-50) at 22 C, with Tris buffer as eluent. CF release from the liposomes

was determined by monitoring the emitted fluorescence at 520 nm from a liposome dispersion (10 mM lipid in 10 mM Tris, pH 7.4). An absolute leakage scale was obtained by disrupting the liposomes at the end of the experiment through addition of 0.8 mM Triton X-100 (Sigma, St. Louis, MO). A SPEX-fluorolog 1650 0.22 m double spectrometer (SPEX Industries, Edison, NJ) was used for the liposome leakage assay. Measurements were performed at 37 C.

CD Spectroscopy. The CD spectra of the peptides in solution were measured on a Jasco J-810 spectropolarimeter (Jasco, U.K.). The measurements were performed at 37 C in a 10 mm quartz cuvette under stirring, and the peptide concentration was 10 μM. The effect on peptide secondary structure of liposomes at a lipid concentration of 100 μM was monitored in the range 200−250 nm. The only peptide conformations observed under the conditions investigated were α-helix and random coil. The fraction of the peptide in α-helical conformation, X_α, was calculated from

$$X_\alpha = (A - A_c)/(A_\alpha - A_c)$$

where A is the recorded CD signal at 225 nm and A_α and A_c are the CD signal at 225 nm for a reference peptide in 100% α-helix and 100% random coil conformation, respectively. 100% α-helix and 100% random coil references were obtained from 0.133 mM (monomer concentration) poly(L-lysine) in 0.1 M NaOH and 0.1 M HCl, respectively (*36, 37*). For determination of effects of lipopolysaccharide on peptide structure, the peptide secondary structure was monitored at a peptide concentration of 10 μM, both in Tris buffer and in the presence of *E. coli* lipopolysaccharide (0.02 wt %) (*E. coli* 0111:B4, highly purified, less than 1% protein/RNA; Sigma, U.K.). To account for instrumental differences between measurements, the background value (detected at 250 nm, where no peptide signal is present) was subtracted. Signals from the bulk solution were also corrected for.

QSAR Analysis of Peptide Activities. The peptide sequence dependent QSAR modeling was performed using ProPHECY, a proprietary software from SARomics AB, Lund, Sweden (www.saromics.com). This software contains >100 descriptors specifically adapted for both peptide and protein design. Typically, both global (e.g., net charge, net hydrophobicity) and local (e.g., amino acid principal properties (*38*)) descriptors are included. The method uses PLS regression in order to correlate the experimental activity with the descriptors, which were subjected to unit-variance scaling and mean centering. In the design of peptide variants 99−117 using ProPHECY all previous peptides (1−98) were used in each model; thus the models were not trimmed by deletion of particular peptides.

Prediction of Helix Propensity and Other Calculations. An algorithm based on helix−coil transition theory, AGADIR, was used to predict helical propensity (*28*). Calculations were performed through the AGADIR service at the EMBL WWW gateway AGADIR (http://www.embl-heidelberg.de/Services/serrano/agadir/agadir-start.html). Input parameters were as follows: Cterm free, Nterm free, pH 7.4, temperature 278 K, and ionic strength 0.15 M. Amphipathicity was investigated by generating helical wheel diagrams. Relative hydrophobic moment (μHrel) was calculated using the web-based algorithm found at http://www.bbcm.univ.trieste.it/~tossi/HydroCalc/HydroMCalc.html.

RESULTS

Structural Considerations, Design, and Initial Evaluation of Peptide Variants. Previous X-ray crystallographic studies of human C3a anaphylatoxin have shown that the C-terminal segment (CNYITELRRQHARASHLGLAR) adopts an α-helical conformation when part of the holoprotein (*39*), where the helix ends at G18 in the peptide. As an isolated peptide, on the other hand, this region adopts a dynamic random coil conformation in aqueous solution. Nevertheless, the peptide has the ability to adopt a helical conformation in specific solvent environments, such as the presence of TFA (*40, 41*) or bacterial lipopolysaccharide (LPS) (*26*). For the initial antimicrobial screening studies, a PEP screen library composed of the 20mer peptide CNYITELRRQHARASHLGLA and its variants (CNY-peptides) was used. This peptide shows a preserved antibacterial activity when compared to the endogenous 21 aa peptide (*22*), despite lacking the C-terminal arginine residue. In Figure 1A, the 20 aa peptide (hereafter denoted peptide 1) is modeled to adopt an α-helical conformation, and possible interactions are depicted (one-letter amino acid designations and their respective position in the peptide are indicated). For example, the side chains of R9 and Q10 may form hydrogen bonds to the side chain of E6, while the side chain of R13 may form a hydrogen bond to the side chain of Q10, both stabilizing the helical conformation. Helix content in the peptide is drastically increased by insertion of preferred N-cap and C-cap motifs, as well as by optimization of the spacing of hydrophobic residues in the peptide. A spacing of i, $i + 3$ or i, $i + 4$ especially between leucines is known to stabilize helices with the latter spacing giving the strongest interaction (*42*). In this context, it is worth noting that Y3 and I4 contribute to favorable i, $i + 4$ and i, $i + 3$ interactions, respectively, with L7 in the N-terminus of the C3a peptide. For example, the predicted helix content (using AGADIR) is increased from 5% to almost 50% by inserting leucine residues at positions 8, 11, 12, and 16. Considering cationicity, it is noteworthy that variation in net charge correlates to antimicrobial activity of the C-terminal region of C3a and related peptides during evolution (*26*). Likewise, a disproportionate alteration of charge appears to characterize the evolution of β-defensins (*43*) and the primate cathelicidin (*6*). These evolutionary clues, combined with the structural considerations above, facilitated the design of new peptide variants with increased positive net charge, high helicity, and improved amphipathicity. The amino acid alterations are illustrated in Figure 1B, whereas peptide sequences are given in Figure 2. The different design strategies used for the various peptides are outlined in Table 1. Figure 2 illustrates antimicrobial effects of peptides against *E. coli*, *S. aureus*, and *C. albicans,* as well as hemolysis, in relation to net charge, predicted helical propensity, and the hydrophobic moment (assuming a helical conformation) of the peptides. Among the first 20 peptides, which were designed to increase helicity by stabilization of N-cap and C-cap motifs, relatively few displayed any enhancement of antimicrobial effects. Peptides with net charge +3 (i.e., peptide 12) as well as increased hydrophobicity (peptides 18−23) displayed significantly increased RDA values against *E. coli*. In general, peptides with optimized amphipathic structure demonstrated high RDA values against *E. coli* (peptides 30, 31, 33, and 34). However,

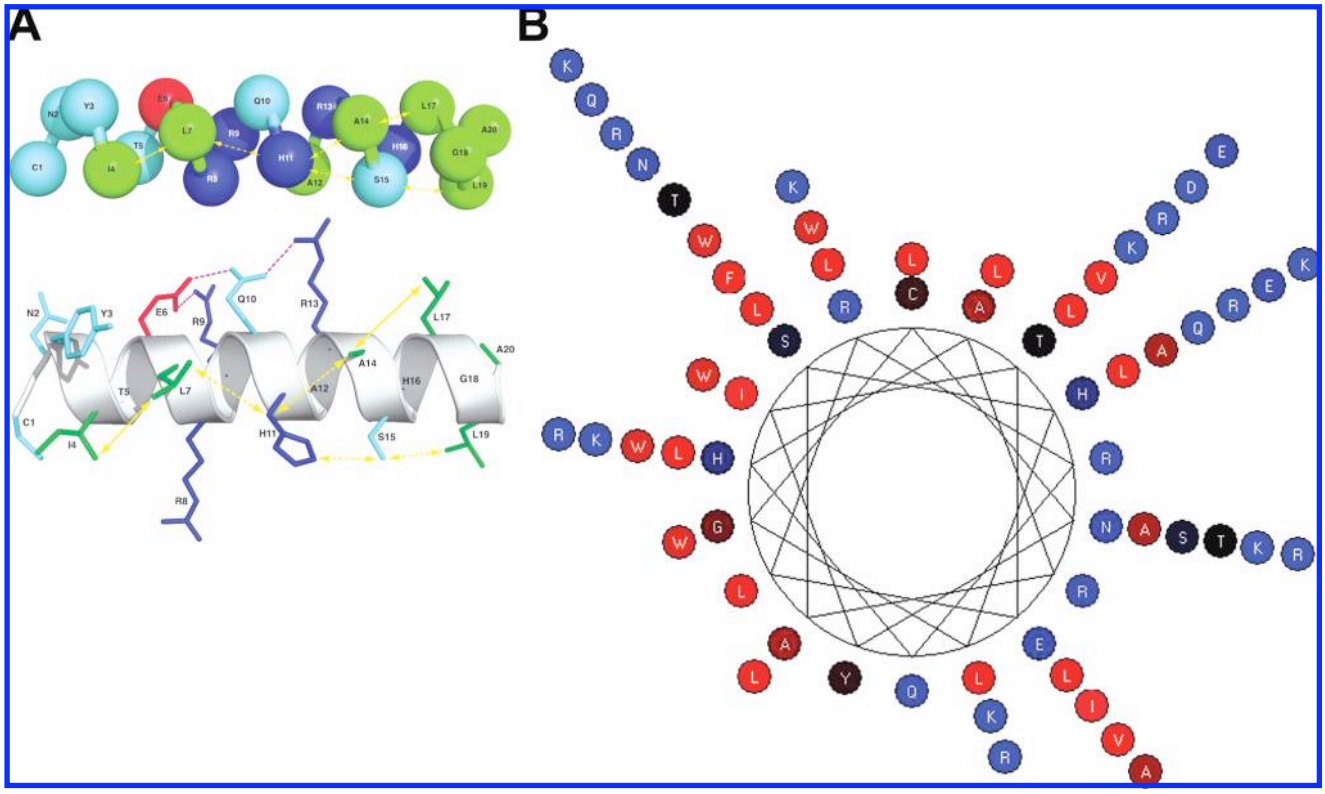

FIGURE 1: Structure and sequence variations. (A) Space-filling model of the native CNY peptide (no. 1) CNYITELRRQHARASHLGLA arranged as an α-helix (upper, space filling model; lower, side chains depicted). Dashed lines (magenta) indicate possible hydrogen bonds and ionic interactions discussed in the text. Yellow arrows outline the existing and induced (dashed arrows) hydrophobic side of the peptide making up the amphiphathic character. The one-letter amino acid designations and their respective position (R8, H11, etc.) are used throughout the text. (B) A helical wheel (Edmundson) projection of the peptide. The innermost amino acids represent the native structure. The outer amino acids indicate the modifications introduced (see Figure 2 for sequences). The amino acids are indicated.

peptides 33 and 34, predicted to have a high helical content, also displayed a hemolytic activity. Correspondingly, peptides 35−45 (except 38) which had combined substitutions to maximize helicity demonstrated a high hemolytic activity. In order to decrease hemolytic activity, a second round of peptides was designed with less optimal amphipathicity. Peptides were designed to have enhanced amphipathicity in the N- and C-terminus or a break of amphipathicity in the central region (Table 1, Figure 2). Almost all peptides tested displayed significant antimicrobial effects against *E. coli*, and several were also effective against *S. aureus*. No obvious differences were detected for the different peptide groups having breaks in amphipathicity at the N-terminus, C-terminus, or central regions (Figures 1B and 2). Particularly, peptides 62−84 showed high antimicrobial activity against *E. coli*. Furthermore, the results indicate that peptides with imperfect amphipathic structures, carrying also a high net charge, are preferably active on both *S. aureus* and *Candida* species.

QSAR Analysis of Peptide Activities. Sequence-dependent QSAR models based on the data for peptides 1−98 were developed for *S. aureus*, *C. albicans*, and *E. coli*, as well as peptide-induced hemolysis using the software ProPHECY (Figure 1, Supporting Information). The squared correlation for the fitted data, r^2, the cross-validated data, q^2, and the number of PLS components, *A*, are given for each model (see figure legends). A moderate q^2 equal to 0.42 was obtained for *S. aureus*, and a similar result was noted for *E. coli.* Considerably higher values, around 0.75, were obtained for *C. albicans* and for hemolysis. The QSAR model for the *S. aureus* activity was used in order to design new peptides with high predicted activities. Around 1000 virtual peptide sequences were hereby constructed, and their activity was predicted using the previously created model. From the virtual library, peptides 99−117, having predicted high activities against *S. aureus* (Figure 1, Supporting Information), were selected for synthesis and testing. The high activity of the new peptides (Figure 2) showed that this procedure resulted in a successful selection of peptides. Regressions based on the results for *all* peptides 1−117 were performed in order to evaluate whether the added data could improve the models, particularly for *S. aureus* and *E. coli*. The new models for *S. aureus* and *E. coli* yielded $q^2 = 0.74$ and 0.55, respectively, which is considerably higher than obtained with the previous models (Figure 1, Supporting Information). As before, the models for *C. albicans* and for hemolysis yielded high values of q^2, 0.76 and 0.78, respectively. One reason for the improved models, particularly for *S. aureus*, is the inclusion of several more highly active peptides. The observed and predicted activities for peptides 1−117 are shown in Figure 3. Additional analyses (correlation plots) utilizing the data presented in Figure 2 showed that AMPs of low and intermediate helical propensities, as judged by the AGADIR predictions, yielded antimicrobial effects on both *E. coli* and *S. aureus* as well as *C. albicans* (Figure 2A, Supporting Information). A significant correlation to the product of net charge and hydrophobic moment was detected for the hemolytic activity (Figure 2B, Supporting Information). In contrast to the results with *E. coli*, the RDA values for *S. aureus* ($r^2 = 0.72$) and *Candida* correlated

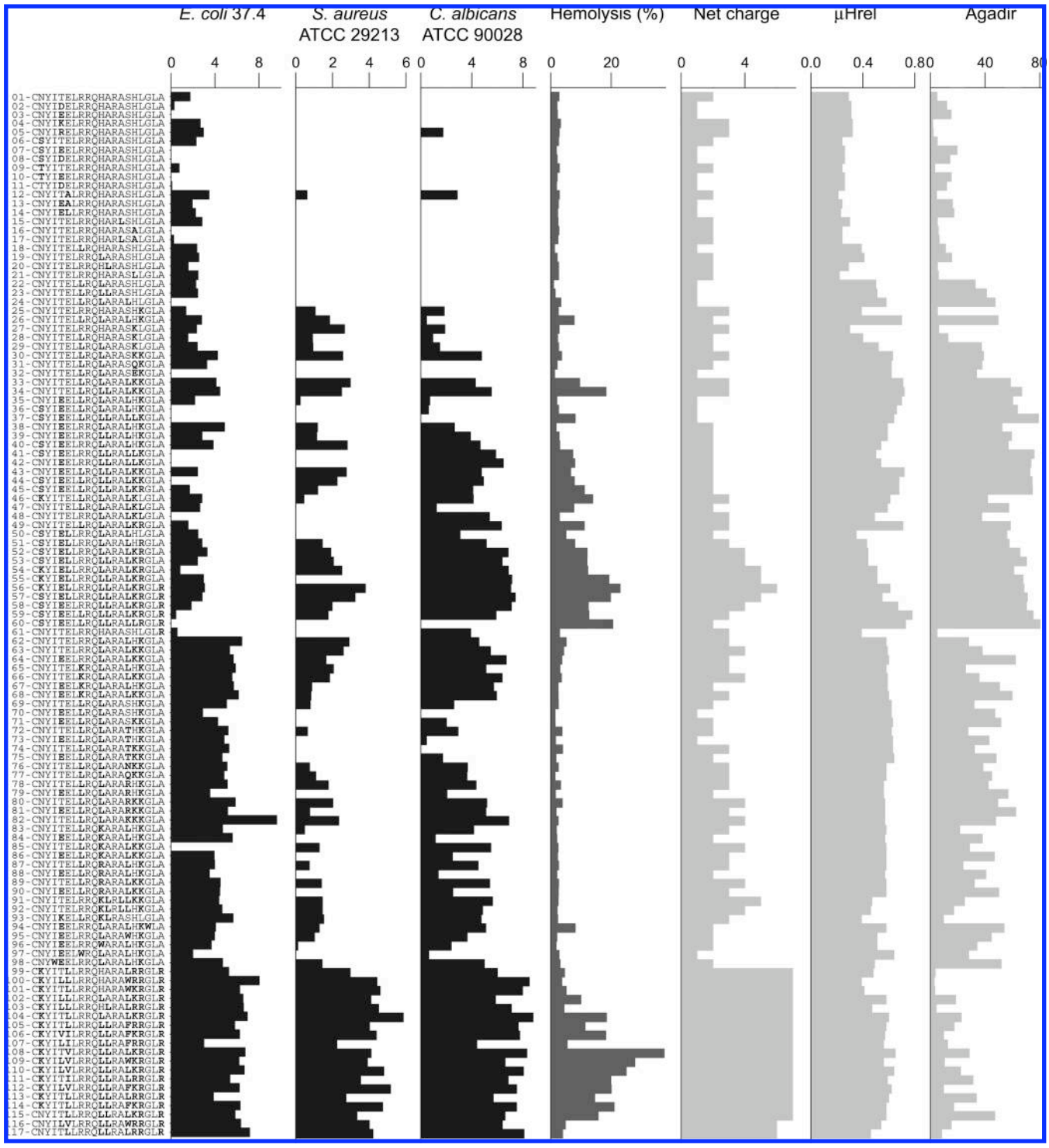

FIGURE 2: Activities and biophysical data of peptides. A composite figure indicating numbered peptide sequences, antimicrobial activity against *E. coli* 37.4, *S. aureus* ATCC 29213, and *C. albicans* ATCC 90028 (black bars), hemolysis (in %), relative hydrophobic moment (μHrel), net charge, and predicted helical propensity (AGADIR). For determination of antimicrobial activities, *E. coli* 37.4, *S. aureus* ATCC 29213 isolates (4×10^6 cfu) or *C. albicans* ATCC 90028 (1×10^5 cfu) was inoculated in 0.1% TSB agarose gel. Each 4 mm diameter well was loaded with 6 μL of peptide (at 100 μM). The zones of clearance correspond to the inhibitory effect of each peptide after incubation at 37 C for 18−24 h (mean values are presented, $n = 3$).

strongly to net charge (Figure 2A, Supporting Information). Despite this, it would be insufficient to use net charge alone as a guide for optimization as there are evidently also contributions related to hydrophobicity and amphipathicity. It is also of interest to note that the activity for *S. aureus* correlates strongly, $r = 0.80$, with the activity for *C. albicans* (Figure 3, Supporting Information), while there is a low correlation with *E. coli* and the logarithm of the hemolytic activity ($r = 0.69$ and 0.56, respectively).

Evaluation of Antimicrobial and Hemolytic Activities of AMPs. Although valuable for the initial evaluation, the PEP libraries contained on average only ~62% pure peptide and, hence, were only used for initial screening purposes and for selection of putative active AMPs. Still, inspection of the

Table 1: Design Strategies

structural feature	peptide position	design criteria	peptide no.
First Set			
N-terminal capping box	2, 5−6	increase helicity	2−14
C-terminal capping box	14, 16	increase helicity	15−17
leucine spacing	8, 11−12, 16	increase helicity	18−23
amphipathicity	8, 11−12, 15−17	improve amphipathicity	24−34
combinations of above features	2, 5, 8, 11−12, 15−17	optimization	35−45
net positive charge	2, 5−6, 8, 11−12, 15−17, 20	increase positive charge	46−61
Second Set			
amphipathic C-terminal	5, 8, 11, 15−17	nonoptimal amphipathicity	62−68
amphipathic N-terminal	5, 8, 11, 15−17	nonoptimal amphipathicity	69−82
amphipathic break	5, 8, 11−12, 14−17	nonoptimal amphipathicity	83−93
tryptophan insertion	4−5, 8, 11, 15, 17−18	increase hydrophobicity	94−98

mass spectrometry data showed that contaminants consisted of smaller peptides, likely being truncated version of the major peptide of relatively minor effect on the observed antimicrobial activity (*34, 35*). The demonstration that antimicrobial activity is dependent on peptide length, shorter truncated peptides being significantly less active (*34*), together with a good agreement of experimental data for peptides of specific structural groups (charge, amphipathicity, predicted helicity) therefore clearly indicates the usefulness of these initial data. Nevertheless, based on the data obtained from the initial screening, a series of highly pure (>95%) peptides were synthesized and further analyzed (Figure 4A). These included additional (peptides 118−122) *in silico* constructed peptides based on the existing QSAR model with high predicted activity against *S. aureus.*

Antimicrobial assays confirmed the high activity of these peptides, when compared to the benchmark peptide LL-37 on *S. aureus*, *C. albicans*, and *E. coli* (Figure 4A). The *in silico* selected peptides also displayed (with the exception of 121) little hemolytic effect. A good agreement was also demonstrated for hemolysis and human keratinocyte (HaCat) permeabilization (Figure 4A and B), indicating that hemolysis could serve as a sufficient and suitable variable for assessing cell toxicity. Analogously, a reciprocal relationship was noted for cell permeabilization and cellular viability (Figure 4A). A subset of these peptides were analyzed on nine different, genotypically distinct clinical *S. aureus* isolates derived from patients with atopic dermatitis (Figure 4C). Compared to the native C3a-derived peptide, the designed peptides presented MIC values[2] that were comparable to or lower than those obtained for the benchmark peptide LL-37. On the basis of these results, we selected two peptides (100 and 122) for further analysis. In order to test the importance of the central histidine residue (H11), which is highly conserved in vertebrates (*26*), peptide variants having H replaced by L were synthesized and analyzed (Figure 5A). As demonstrated by RDA and dose−response experiments, the four peptide variants displayed similar activities on *S. aureus* and *C. albicans*, whereas the H-L variants were slightly less active against *E. coli* (Figure 5B). In correspondence with the RDA results presented in Figure 4A, the modified peptides permeabilized *S. aureus,* in contrast to the original peptide 1 (Figure 5C). It was noted that the leucine-substituted peptides (100H-L and 122H-L) were highly hemolytic (Figure 5D), which was paralleled by an increase in cell-permeabilizing activity (Figure 5E, upper panel) and decrease in cellular viability (Figure 5E, lower panel). An additional QSAR model using ProPHECY based on peptides 1−122 was constructed in order to predict the properties of the H-L variants. The activity changes were in good agreement with the experimental observations. For both variants the model predicted a slight increase in the activity against *S. aureus* and *C. albicans* and an insignificant decrease in activity against *E. coli*. Furthermore, the hemolysis was predicted to increase by a factor of 2 compared to peptides 100 and 122, respectively (not shown).

For illustrative purposes we constructed also simplified QSAR models for *S. aureus*, *C. albicans*, *E. coli*, and hemolysis using all 122 peptides but only three computed variables, i.e., net charge, AGADIR, and the mean hydrophobicity per residue (using the scale of Chen et al. (*9*)) (Figure 6). The variables had small pairwise correlations, ranging from $r = -0.30$ to $r = 0.39$. We point out that these simple QSAR equations were not used during the optimization and hence are only presented in order to simplify an interpretation of the experimental results. The PLS technique was used, and as before the variables were subjected to mean centering and scaling to unit variance, and the number of components was determined by cross-validation. In spite of using only three descriptors, the models capture most of the variation in the experimentally determined activities. Figure

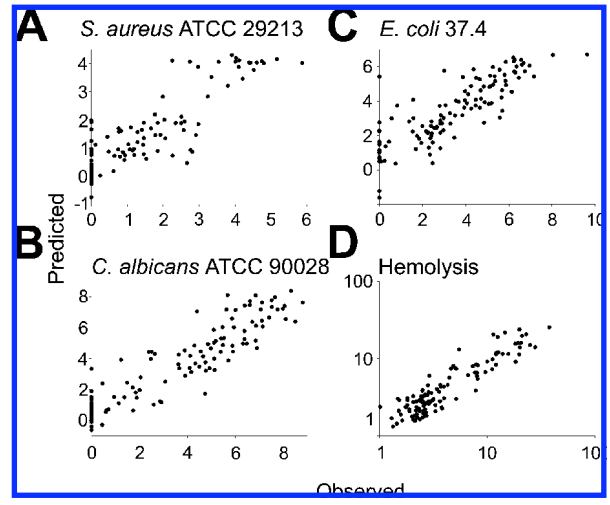

FIGURE 3: QSAR analyses. QSAR models for the experimental versus predicted values for the set of C3a-derived peptides (1−117). Antimicrobial activities: (A) *S. aureus*, $r^2 = 0.77$, $q^2 = 0.74$, and $A = 3$, (B) *C. albicans*, $r^2 = 0.84$, $q^2 = 0.76$, and $A = 4$, (C) *E. coli*, $r^2 = 0.70$, $q^2 = 0.55$, and $A = 4$, and (D) hemolytic activity against human erythrocytes, $r^2 = 0.84$, $q^2 = 0.78$, and $A = 4$.

[2] The standard MIC method according to CLSI (formerly NCCLS) was modified; for details see Experimental Procedures.

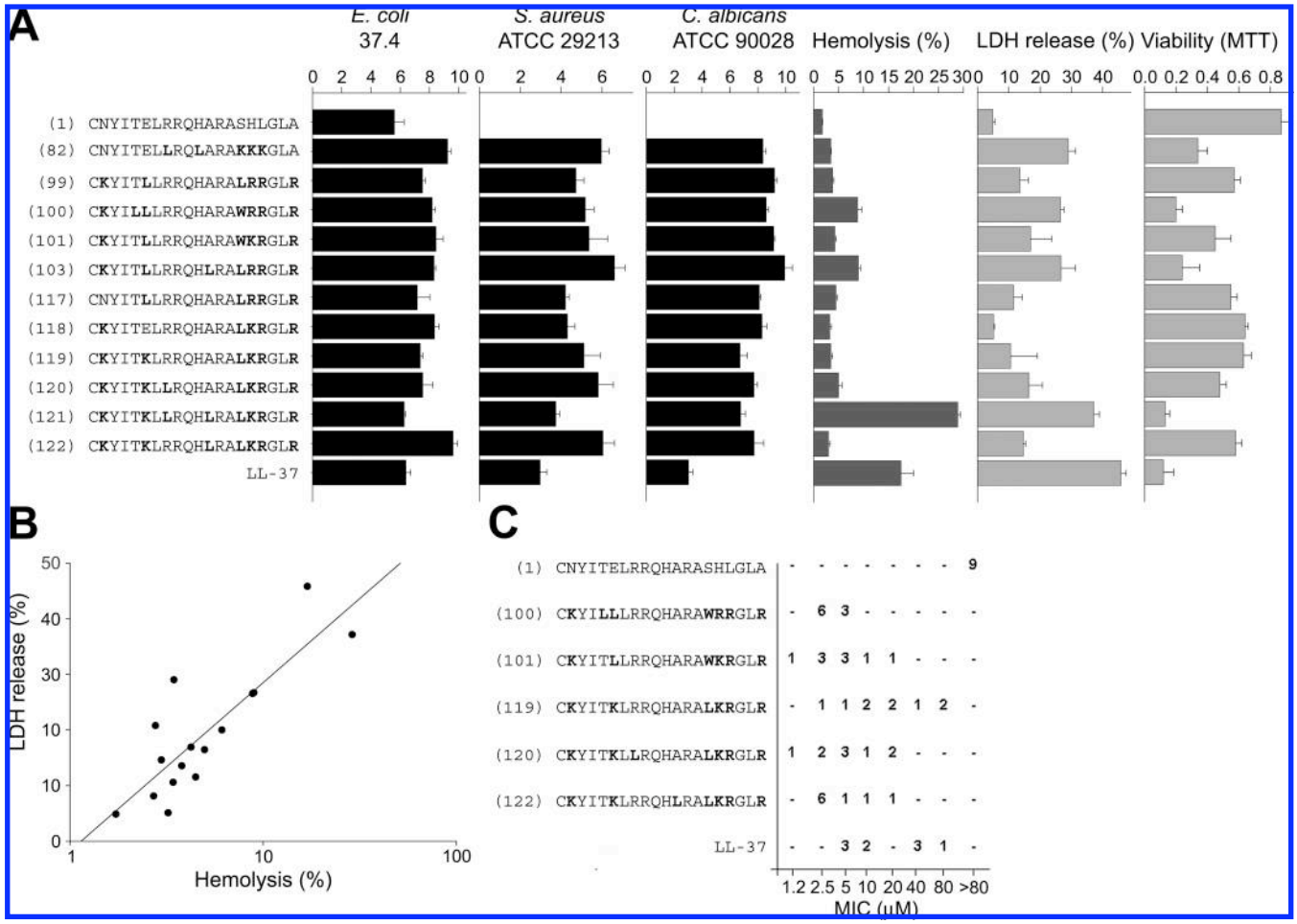

FIGURE 4: Activities of selected peptides. (A) Antimicrobial activity of selected peptides (at 100 μM in RDA) against *E. coli* 37.4, *S. aureus* ATCC 29213, and *C. albicans* ATCC 90028, hemolysis (in %), and LDH release and viability (MTT) of a human keratinocyte cell line subjected to the indicated peptides at 60 μM. (B) Relation between hemolysis of human erythrocytes and permeabilizing activity on human HaCat cells. (C) Minimum inhibitory concentrations of indicated peptides against nine different *S. aureus* isolates (of which eight were clinical isolates from atopic dermatitis patients).

6 graphically illustrates the coefficients of the variables in the different QSAR models. Strikingly, there is a pronounced difference between the model for the hemolysis and the antimicrobial activities. Thus, the former model has a dominant contribution from the mean hydrophobicity, but there is also a substantial contribution from the net charge and a smaller contribution from AGADIR. The coefficients for all variables are positive so that large and positive values of all of these variables contribute toward a predicted high hemolytic activity. The models for the antimicrobial activities, on the other hand, are all dominated by the positive coefficient for the net charge. In particular for *S. aureus* this variable completely dominates the predicted activity. The models for *C. albicans* and *E. coli* both have coefficients that are negative for mean hydrophobicity and positive for AGADIR while the magnitude of the coefficients is different (see Table 1, Supporting Information, for equations).

Application of the simplified QSAR models (Figure 6) to the H-L substituted variants of peptides 100 and 122 shows that the models capture much of the observed effects. As the substitutions do not result in any change in net charge, the predicted effects are due to changes in hydrophobicity and/or AGADIR. The hemolysis, in turn, is predicted to increase by about 45−60%, due mostly to the increase in hydrophobicity upon H-L substitution. Moreover, the model for *S. aureus* predicts that the H-L substitutions only result in very slight activity changes, a consequence of the small magnitude of the coefficients for AGADIR and hydrophobicity. In comparison, the *E. coli* model predicts a decrease in activity for the H-L substituted peptides by about 0.5 unit, in qualitative agreement with the experimental observation. The increase in hydrophobicity upon replacement of H with L, in combination with a negative coefficient for the hydrophobicity, is responsible for the majority of the decrease in predicted activity. The situation is more complex for the *C. albicans* predictions. In this case the contributions from both AGADIR and hydrophobicity can substantially influence the predicted activity (Figure 6). The equation has a positive coefficient for AGADIR and a negative coefficient for hydrophobicity. Due to contributions of similar magnitudes but of opposite sign from AGADIR and hydrophobicity, the predicted *C. albicans* activity is almost the same for peptides 100 and 100H-L. For peptides 122 and 122H-L, the increase in AGADIR (for peptide 122) is almost twice as compared with the contribution from the change in hydrophobicity. The positive coefficient for AGADIR leads to a predicted net increase in activity of about 0.8 unit. Thus the predictions of the extremely simple QSAR equations are in qualitative agreement with the experimental observations for the influ-

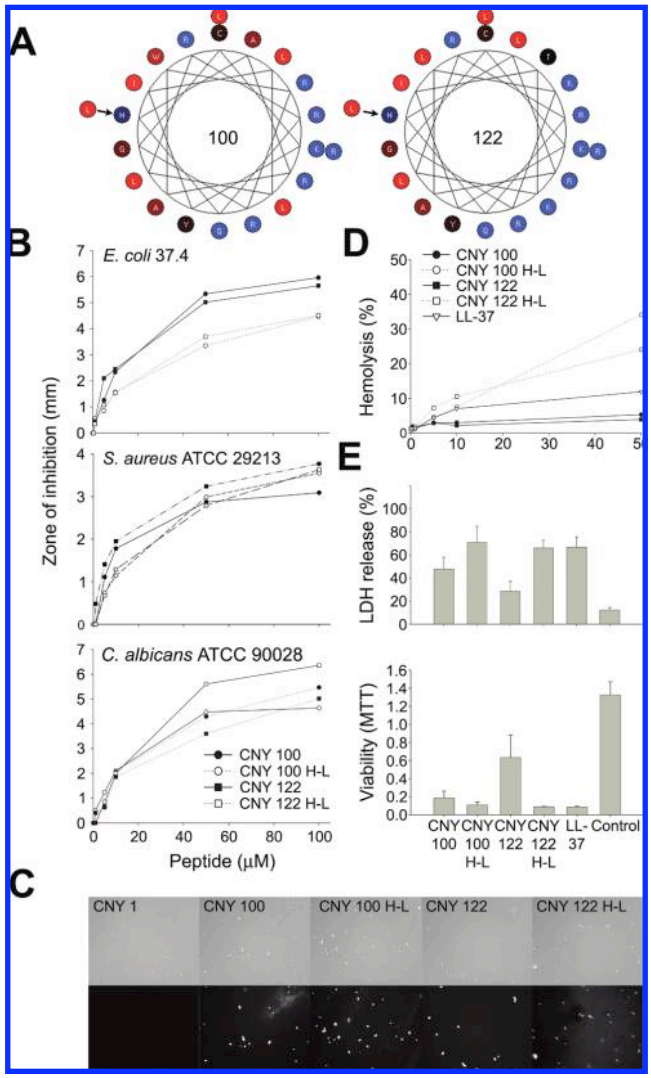

FIGURE 5: Activity of C3a peptide analogues and effects of leucine substitution at position 11. (A) Helical wheel projections of CNY peptides 100 and 122. The position of the H-L substitution is indicated. (B) Antibacterial activities of 100 and 122 peptides and their leucine-substituted variants (100H-L and 122H-L) against *E. coli*, *S. aureus*, and *C. albicans*. The bacteria or *C. albicans* were inoculated in 0.1% TSB agarose gel with different amounts of the peptides. Each 4 mm diameter well was loaded with 6 μL of peptide (at the indicated concentrations). The zones of clearance correspond to the inhibitory effect of each peptide after incubation at 37 C for 18−24 h (mean values are presented, $n = 3$). (C) Permeabilizing effects of peptides on *S. aureus*. *S. aureus* was incubated with the indicated peptides, and permeabilization was assessed using the impermeant probe FITC. (D) Hemolytic effects of peptides 100 and 122 and their H-L variant were investigated. The cells were incubated with different concentrations of the peptides or LL-37; 2% Triton X-100 (Sigma-Aldrich) served as positive control. The absorbance of hemoglobin release was measured at λ 540 nm and is expressed as % of Triton X-100 induced hemolysis (note the scale of the *y*-axis). (E) Upper panel: HaCaT keratinocytes were subjected to the C3a variant peptides and LL-37. Cell permeabilizing effects were measured by the LDH based TOX-7 kit. LDH release from the cells was monitored at λ 490 nm and was plotted as % of total LDH release. Lower panel: The MTT assay was used to measure viability of HaCaT keratinocytes in the presence of the indicated peptides (at 60 μM). In the assay, MTT is modified into a dye, blue formazan, by enzymes associated with metabolic activity. The absorbance of the dye was measured at λ 550 nm.

ence of the H-L substitutions on the changes in hemolytic and antimicrobial activities.

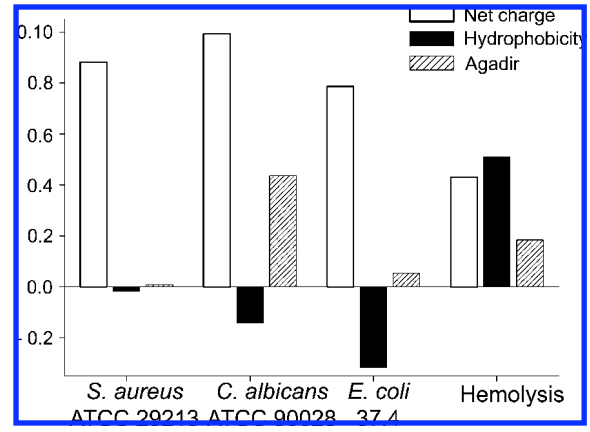

FIGURE 6: Coefficients for the simplified QSAR equations based on peptides 1−122 and the computed variables net charge, helical propensity (AGADIR), and hydrophobicity. The coefficients are given for variables that are mean centered and scaled to unit variance. Antimicrobial activities: (A) *S. aureus*, $r^2 = 0.76$, $q^2 = 0.73$, and $A = 2$, (B) *C. albicans*, $r^2 = 0.79$, $q^2 = 0.77$, and $A = 2$, (C) *E. coli*, $r^2 = 0.49$, $q^2 = 0.46$, and $A = 2$, and (D) logarithm of the hemolytic activity against human erythrocytes, $r^2 = 0.66$, $q^2 = 0.65$, and $A = 1$. The full equations are given in the Supporting Information.

Membrane Permeabilization and Structural Studies. In order to obtain further structural and mechanistic information on the mode of action of the above peptide 100 and 122 variants, CD measurements were performed in buffer as well as in the presence of bacterial LPS (Figure 7A and Figure 4, Supporting Information) or liposomes (Figure 7B). As exemplified in Figure 7A,B, the α-helix content for the peptides is low in buffer, with random coil as the dominating conformation. LPS induced a conformational change in peptide 100 (Figure 7A), and to a greater extent in the leucine-substituted variant, 100H-L (Figure 7A). Similar results were obtained using the peptide 122 variants (Figure 4, Supporting Information). In analogy, addition of anionic liposomes significantly affected helix content for the 100H-L and 122H-L peptides (Figure 7B). In this context it should be noted that CNY21 has previously been observed to form a helical conformation in TFA (*40, 41*), which may indicate that caution should be taken when using TFA or other solvents as models for the lipid membrane environment. The four modified C3a peptides showed significantly higher membrane disruptive effects on liposomes when compared with the native peptide, and notably, the H-L variants were the most active (Figure 7C), likely reflecting their increased hydrophobicity and helix-inducing capability in an membrane environment. The similar leakage induction observed for the zwitterionic and the anionic liposomes indicates that the membrane disruptive effects are not drastically affected by the magnitude of the negative electrostatic potential in the range −10 mV (zwitterionic liposomes) to −30 mV (anionic liposomes). This is in line with previous observations of semiquantitatively similar effects of peptide modifications such as length, charge, hydrophobicity, and topology are obtained for zwitterionic and anionic phospholipids membranes (*33, 34*). Having said that, it must of course be recognized that isolated model systems (those used here or other model lipid systems not composed of the complete lipid composition, as well as membrane bound proteins, glycoproteins, etc.) do not reflect the complex interactions taking place at bacterial surfaces. Nevertheless, it is clear that the

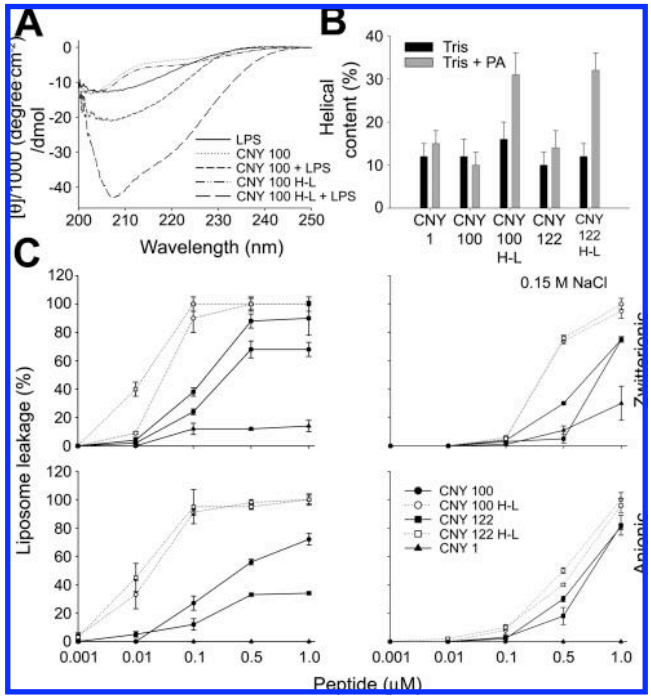

FIGURE 7: CD analysis and permeabilization of liposomes. (A) CD spectra of CNY peptide 100 and 100H-L in Tris buffer and in the presence of LPS. For control, CD spectra for buffer and LPS alone are also presented. (B) Helical content of the indicated peptides in the presence of negatively charged liposomes (PA). The two peptides 100H-L and 122H-L showed a marked helix induction upon addition of the liposomes. (C) Effects of the indicated peptides on liposome leakage. The membrane permeabilizing effect was recorded by measuring fluorescence release of carboxyfluorescein from liposomes. Upper panels show PC-containing (neutral) liposomes, and lower panels show PA (negatively charged) liposomes. Left panels indicate results obtained in 10 mM Tris buffer, whereas right panels show results in buffer with 0.15 M NaCl. Values represent mean of triplicate samples.

peptides induce membrane disruption as well as bactericidal activity, suggesting that breakdown of bacterial membranes is at least partly related to disruption of the bacterial lipid bilayer(s).

Together, liposome leakage and CD measurements show that coil → helix transitions are not required for lipid membrane disruption but seem to be related to activity at higher salt conditions and lysis of erythrocyte and eukaryotic cell membranes. This observation was further supported by the finding that the H-L peptides showed improved activity in 0.15 M NaCl in RDA (Figure 8A), when compared with the 100 and 122 peptides. It is notable that peptide 100 still retained activity against *S. aureus* also in 0.15 M NaCl, whereas the benchmark LL-37 was completely inactive against this bacterium (Figure 8A). It is also noteworthy that the divalent cations Mg^{2+} and Ca^{2+} at physiological concentrations (1 mM) and in the presence of 0.15 M NaCl did not inhibit the activity of peptide 100 (Figure 5, Supporting Information). In MIC assays the designed peptides Omiganan (*44*) and Novispirin (*45*), as well as the lipopeptide Polymyxin B (*46*), showed activities against the various *S. aureus* isolates which were comparable to peptide 100 (Figure 5, Supporting Information).

Effects of AMPs in Biological Fluids. Contrasting to the conditions used for most *in vitro* tests for activity and toxicity, blood comprises a complex and protein-rich environment that may affect peptide activity. Notably, the peptide 100 variants required a low concentration for efficient killing of *S. aureus* in the presence of salt as well as plasma (Figure 8B). Interestingly, the H-L variant was significantly more inhibited by plasma (Figure 8B), possibly reflecting a higher affinity to plasma proteins due to its higher hydrophobicity. As demonstrated in Figure 8C, flow cytometry analysis showed that treatment of staphylococci with peptide 100 variants (at physiological salt and presence of plasma) yielded bacteria with permeabilized membranes, thus accessible to influx of the normally impermeant marker propidium iodide. A similar result was obtained with peptide 122 variants (not shown). Although the 100 and 122 variants all killed all bacteria strains investigated under these conditions, there was a particularly increased uptake of propidium iodide after treatment with 100H-L, likely reflecting the increased membrane activity of this peptide variant. It is notable that the native peptide (1) as well as LL-37 was not active against staphylococci in these experiments. Neither the 100 and 122 variants nor LL-37 exhibited any hemolytic or cell-permeabilizing effects in 50% citrate−blood or 20% citrate−plasma, respectively (Figure 8D,E). Taken together, the combination of biophysical experiments, biological data, and *in silico* predictions demonstrates the possibility of identifying C3a peptide analogues with well-defined and graded activities against bacteria and erythrocytes, as well as eukaryotic cells in specific environments. Importantly, the data show that the generated 100 and 122 peptides preserve a specificity for bacterial membranes, even in the presence of plasma and salt, and that the H-L peptide variants, which show high "toxicity" *in vitro*, have an attenuated activity (at similar concentrations) on eukaryotic cells in *in vivo*-like conditions.

DISCUSSION

The present work describes an approach comprising selective amino acid changes based on structural considerations in the human native C3a peptide template, followed by analysis of interdependence of biophysical parameters and antimicrobial as well as hemolytic activity. Using a low number of amino acid substitutions at strategic positions in the original peptide template, peptides were generated exerting a significant activity on *S. aureus*. Overall, the analysis of the substitutions provided information on prerequisites for antimicrobial activity of the C3a analogues. As been found before for other AMPs and bacteria (*2–7*), combinations of a relatively high net charge, a propensity to adopt an α-helical conformation, and an imperfect amphipathicity were identified as important factors for selective antimicrobial activity also for this peptide family. As exemplified with the highly hemolytic C3a analogues having H11 substituted by L, cytotoxic peptides were characterized by high net charge, amphipathicity, and high predicted helicity. In this respect, our data corroborate well with results from other studies on rationally designed α-helical AMPs showing that increased hemolytic activity could derive from both increased cationicity and overall hydrophobicity, as well as from the propensity for helical structuring (*8, 9, 47–50*). In this context it is interesting to note that evolution has favored the selection of antimicrobial C3a peptides showing imperfect hydrophobic regions (assuming a helical conformation). It is also interesting to note

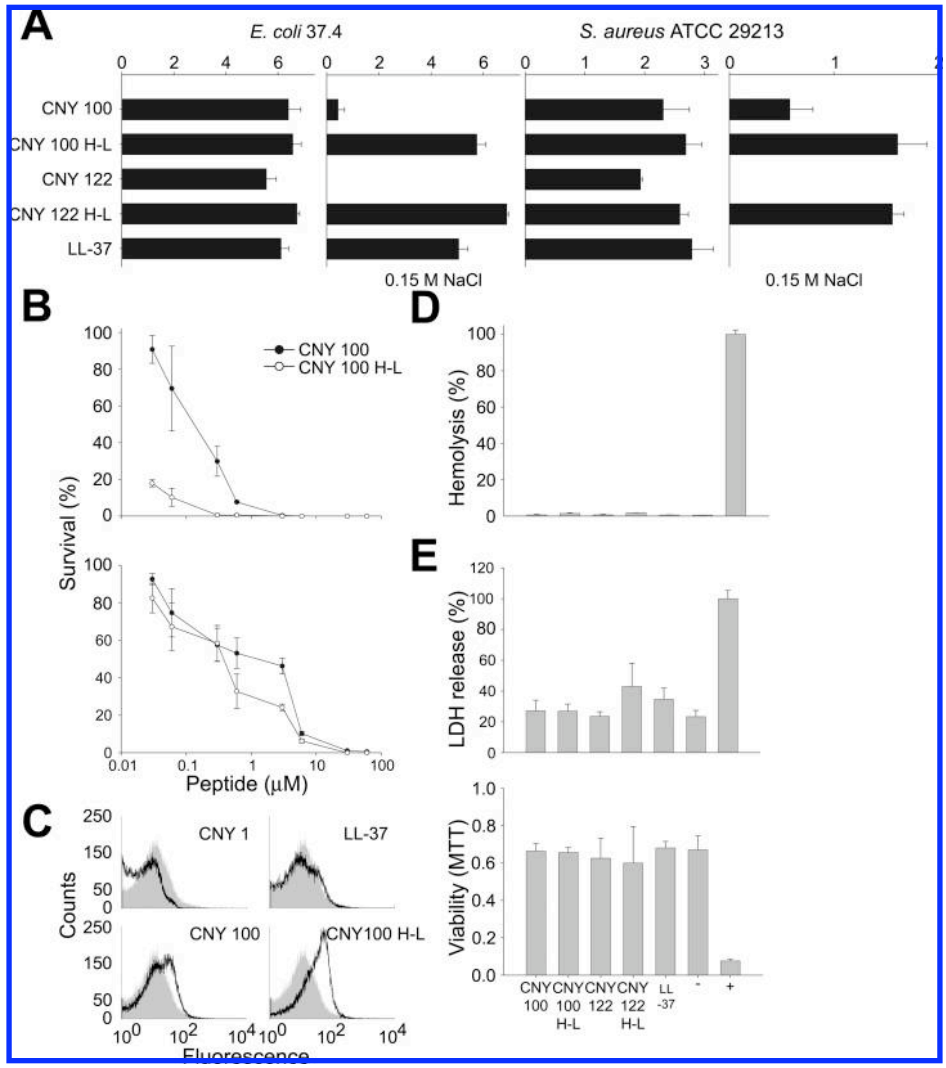

FIGURE 8: Activities of C3a variant peptides and LL-37 at physiological conditions. (A) Peptides were tested in RDA in low-salt conditions and in the presence of 0.15 M NaCl. *E. coli* and *S. aureus* (4×10^6 cfu) were inoculated in 0.1% TSB agarose gel. Each 4 mm diameter well was loaded with 6 μL of peptide at 100 μM. The zones of clearance correspond to the inhibitory effect of each peptide after incubation at 37 C for 18−24 h. (B) In viable count assays, *S. aureus* were subjected to the indicated peptides in 10 mM Tris, pH 7.4, containing 0.15 M NaCl in the absence (upper planel) or presence (lower panel) of 20% human citrate−plasma. Identical buffers without peptide were used as controls. (C) Flow cytometry analysis of *S. aureus* treated with CNY peptides 1, 100, 100H-L, or LL-37. *S. aureus* (1×10^7 cfu/mL) was incubated for 2 h at 37 C in 0.15 M NaCl, 10 mM Tris, pH 7.4, containing 20% plasma with 30 μM peptide 100, 100H-L, or LL-37, respectively, and analyzed by flow cytometry after addition of propidium iodide. (D) Hemolytic effects of peptides (indicated below) in citrate−blood diluted with PBS (1:1) were investigated. The cells were incubated with different concentrations of the peptides or LL-37. 2% Triton X-100 (Sigma-Aldrich) served as positive control. The absorbance of hemoglobin release was measured at λ 540 nm and is expressed as % of Triton X-100 induced hemolysis. (E) Membrane permeabilizing effects (LDH, upper panel) and viability (MTT, lower panel) on HaCat cells in the presence of 20% human plasma.

that R8 is globally conserved among both invertebrates as well as vertebrates and that H11 is found in vertebrates (*26*). These residues induce destructuring (Figure 1A), yielding a low predicted helicity, but as demonstrated here also resulting in a group of optimized C3a peptides, displaying low hemolysis combined with a preserved antimicrobial activity. Similar results have recently been observed for other antimicrobial peptides where detailed experimental analysis showed that stabilization of the α-helical conformation promoted high hemolytic activity (*11*). The C3a variants with H11 substituted by L display a much higher helical content due to establishment of an optimal hydrophobic residue spacing that is otherwise broken by H11 (e.g., for peptide 100: Y3-I4/L6-L7/L11/W15/L19). As observed by Carotenuto et al. (*11*), it is probably the N-terminal stabilization of the helical conformation in 100H-L and 122H-L, which is responsible for the elevated hemolytic activity. In addition, the observation that hemolysis correlates well with epithelial cell permeabilization and thus viability provides a rationale for using hemolysis as a marker for epithelial cell toxicity. Finally, the finding that highly active peptides (the H-L variants) may possess residual toxicity as judged by classical hemolysis assays, but be nontoxic in blood and plasma, illustrates the necessity of taking the environment into account when developing AMPs for various indications. For example, the requirements for tissue compatibility will vary dependent on the locale (mouth, skin, mucous membranes, eyes, etc,) and its salt and protein constituents.

S. aureus displays an impressive number of resistance mechanisms, including net charge alterations (*51, 52*). Thus, the teichoic acid polymers found in the cell wall of this bacterium, as well as in those of other Gram positives,

normally having strong anionic properties mediated by phosphate groups of the glycerophosphate repeating units, can be modified by D-alanine residues with free amino groups. Analogously, the major (and negatively charged) lipid phosphatidylglycerol is modified into a net positive charge by addition of L-lysine (*4, 53*). In relation to this, it is therefore interesting that the present analysis showed that the activity on the Gram-positive bacterium *S. aureus* by the series of peptides strongly correlated with net charge, albeit requiring a sufficient hydrophobicity and amphipathicity. Thus, it is conceivable that the initial electrostatic attraction, which is attenuated by *S. aureus*, may be compensated for by higher charge of the C3a analogues. In this context, it should be added that the designed C3a analogues were all amphipathic as reflected by their mean hydrophobicity (μH), and a content of (spaced) hydrophobic residues, enabling peptide interactions with the bacterial membrane structures. Thus, although the analysis showed that the activity on *S. aureus* by the series of peptides strongly correlated with net charge, it was also dependent on hydrophobicity and amphipathicity, a conclusion supported by the observation that peptides of μH <1 showed no or little activity on this bacterium (see Supporting Information, Figure 2). However, increasing hydrophobicity of highly charged peptides such as exemplified by the H-L variants did not further add to antimicrobial activity against *S. aureus* but, as previously mentioned, instead conferred cytotoxic properties to the peptides. Correspondingly, other studies identify charge as a critical parameter for activity of helical AMPs; decreasing the net charge below $+3$ reduces potency, while increasing the net charge to $+9$ gradually increases activity (*8*). In this context, it is notable that positive selection, disproportionately favoring alterations in the charge, appears to characterize the evolution of β-defensins. Interestingly, hBD3, the human defensin with the highest positive net charge ($+10$), also has the highest activity against *S. aureus* (*54*). Analogous relationships were recently reported to apply to the evolution of primate cathelicidin, showing positive selection affecting charge while keeping hydrophobicity and amphipathicity constant, and as previously mentioned, C3a (*26*). Likely, these observations reflect that evolution has generated AMPs, which control specific bacteriological populations (e.g., certain Gram-negative bacteria), while showing less activity against other bacteria. Indeed, the observation that other AMPs, such as psoriasin, are specific against *E. coli*, while showing little activity against *S. aureus*, is compatible with this reasoning (*55*).

It is well established that structural differences between bacterial, fungal, and mammalian cell surfaces underlie a certain degree of selectivity for AMP action, and many peptides may preferentially target bacteria, fungi, or mammalian cells or combinations thereof (*4, 10*). Thus, bacterial surfaces contain many anionic components, including LPS and anionic lipids of Gram-negative bacteria, as well as teichoic and teichuronic acids of Gram-positive bacteria. Similarly, β-glucan, chitin, mannoprotein, and a blend of other cell wall proteins and polysaccharides contribute to a negative surface potential of fungal surfaces (*56*). Beyond the outer cell surface, AMPs interact with the plasma membrane. Contrasting to eukaryotic membranes, including fungal membranes, which contain mostly zwitterionic lipids (e.g., phosphatidylcholine), bacterial membranes comprise various acidic phospholipids (phosphatidylglycerol, phosphatidylserine, and cardiolipin), which confer a negative charge facilitating AMP binding and sometimes also defect formation (*5, 57*). The plasma membrane of eukaryotic cells contains sphingolipids and sterols, which are missing in prokaryotes (*58*), and which are frequently found to provide some resistance to AMP membrane rupture (*5, 58, 59*). Ergosterol is the major sterol in yeasts, whereas the sterol in plasma membranes of mammalian cells is represented by cholesterol (*58*). It has also become increasingly clear that AMP selectivity may also depend on factors such as AMP oligomerization and preassembly (in solution and membrane) (*60*). Clearly, all of these factors contribute to AMPs exhibiting different activity spectra on bacterial and fungal membranes, as well as toxicity on eukaryotic cells. Hypothetically, all of this complexity should correspond to different activity profiles of individual peptides, reflecting the different physicochemical properties of microbes as well as peptide behavior in solution. Using the H-L variants as an example, a change of one critical amino acid induces a striking selectivity change, i.e., the peptide increases its affinity for eukaryotic membranes. Considering the whole group of C3a analogues, peptides characterized by intermediate charge ($+2$ to $+3$) as well as helicity showed activity on *E. coli,* whereas those having moderate charge and a high predicted helicity were preferably acting on *C. albicans*. In this context, it is noteworthy that the activity against staphylococci appeared to correlate well with activity against the yeast *C. albicans*. The observation that there was no clear association between activity of the Gram-negative *E. coli* and the Gram-positive *S. aureus*, as well as hemolysis, further underscores that subtle peptide changes address different physicochemical relationships of microbes and eukaryotes. Furthermore, the correlation between activity of *S. aureus* and *C. albicans* suggests that these organisms must share common physicochemical properties recognized by this family of C3a analogues. Application of sequence-dependent QSAR models has previously been in use for assessing antimicrobial activity on single (*18, 61, 62*) or two bacterial species (*63*). Interestingly, the latter study showed that differences in antibacterial activities of AMPs reflect different properties of the target membranes, an observation which is compatible with the results presented here for the C3a peptide analogues and also a two-state model that explains the action of both helical and β-sheet antimicrobial peptides after they bind to the plasma membranes of cells (*64*). In the present work, utilization of QSAR models aided in the further generation of active C3a analogues, and as demonstrated here, the models were also helpful in the generation and prediction of C3a analogues of low hemolysis as well as high activity against *S. aureus*, demonstrating that QSAR analyses could be a valuable tool aiding in the design of novel peptide analogues with altered activity spectra. It is notable that analogously to the conclusions reached above, based on structural reasoning and "two-dimensional" data, a correspondence was observed with the QSAR analyses. For example, the simplified QSAR models with only three global descriptors showed that the increase in mean hydrophobicity (μH) was responsible for a major part of the predicted increase in hemolysis. Although this study, as well as work of others (*63*), indicates the existence of specific peptide−microbe interactions governing activity spectra

against different microbial species (e.g., Gram-positive and Gram-negative bacteria), it should also be considered that the results are based on a limited number of organisms. Thus, the possibility exists that intraspecies variations may account for some of the differences observed. For example, although peptide 100 showed a narrow MIC range against different *S. aureus* isolates, other peptides (e.g., 119; see Figure 4C) as well as the benchmark LL-37 exhibited MICs between 5 and 80 μM. Clearly, the differences in spectra vis-à-vis Gram-positive, Gram-negative bacteria, fungi, and eukaryotic cells noted here for various C3a analogues, and their relation to both classical descriptive features (AGADIR, μH, net charge, etc.) as well as QSAR model differences need further verification using a selected set of C3a analogues and additional bacterial as well as fungal isolates. This is currently addressed and is well beyond the scope of this work. Nevertheless, our results point at the interesting possibility of developing peptides that specifically target selected microbial populations. From an ecological perspective, this approach could have therapeutical advantages, leading to preservation of the normal bacterial flora.

ACKNOWLEDGMENT

We thank Ms. Mina Davoudi, Ms. Lise-Britt Wahlberg, and Ms. Oonagh Shannon for valuable support and input.

SUPPORTING INFORMATION AVAILABLE

QSAR analyses, correlation plots, CD spectroscopy data, antimicrobial assays in the presence of Ca^{2+} and Mg^{2+}, MIC comparison with benchmark AMPs, and equations for the simplified QSAR models. This material is available free of charge via the Internet at http://pubs.acs.org.

REFERENCES

1. Tlaskalova-Hogenova, H., Stepankova, R., Hudcovic, T., Tuckova, L., Cukrowska, B., Lodinova-Zadnikova, R., Kozakova, H., Rossmann, P., Bartova, J., Sokol, D., Funda, D. P., Borovska, D., Rehakova, Z., Sinkora, J., Hofman, J., Drastich, P., and Kokesova, A. (2004) Commensal bacteria (normal microflora), mucosal immunity and chronic inflammatory and autoimmune diseases. *Immunol. Lett. 93*, 97–108.
2. Powers, J. P., and Hancock, R. E. (2003) The relationship between peptide structure and antibacterial activity. *Peptides 24*, 1681–1691.
3. Bulet, P., Stocklin, R., and Menin, L. (2004) Anti-microbial peptides: from invertebrates to vertebrates. *Immunol. Rev. 198*, 169–184.
4. Yount, N. Y., Bayer, A. S., Xiong, Y. Q., and Yeaman, M. R. (2006) Advances in antimicrobial peptide immunobiology. *Biopolymers 84*, 435–458.
5. Durr, U. H., Sudheendra, U. S., and Ramamoorthy, A. (2006) LL-37, the only human member of the cathelicidin family of antimicrobial peptides. *Biochim. Biophys. Acta 1758*, 1408–1425.
6. Zelezetsky, I., Pontillo, A., Puzzi, L., Antcheva, N., Segat, L., Pacor, S., Crovella, S., and Tossi, A. (2006) Evolution of the primate cathelicidin—correlation between structural variations and antimicrobial activity. *J. Biol. Chem. 281*, 19861–19871.
7. Tossi, A., Sandri, L., and Giangaspero, A. (2000) Amphipathic, α-helical antimicrobial peptides. *Biopolymers 55*, 4–30.
8. Zelezetsky, I., and Tossi, A. (2006) α-Helical antimicrobial peptides—Using a sequence template to guide structure-activity relationship studies, *Biochim. Biophys. Acta*.
9. Chen, Y., Mant, C. T., Farmer, S. W., Hancock, R. E., Vasil, M. L., and Hodges, R. S. (2005) Rational design of α-helical antimicrobial peptides with enhanced activities and specificity/therapeutic index. *J. Biol. Chem. 280*, 12316–12329.
10. Papo, N., and Shai, Y. (2003) Can we predict biological activity of antimicrobial peptides from their interactions with model phospholipid membranes? *Peptides 24*, 1693–1703.
11. Carotenuto, A., Malfi, S., Saviello, M. R., Campiglia, P., Gomez-Monterrey, I., Mangoni, M. L., Gaddi, L. M., Novellino, E., and Grieco, P. (2008) A different molecular mechanism underlying antimicrobial and hemolytic actions of temporins A and L. *J. Med. Chem. 51*, 2354–2362.
12. Hawrani, A., Howe, R. A., Walsh, T. R., and Dempsey, C. E. (2008) Origin of low mammalian cell toxicity in a class of highly active antimicrobial amphipathic helical peptides, *J. Biol. Chem.*
13. Jiang, Z., Vasil, A. I., Hale, J. D., Hancock, R. E., Vasil, M. L., and Hodges, R. S. (2008) Effects of net charge and the number of positively charged residues on the biological activity of amphipathic α-helical cationic antimicrobial peptides. *Biopolymers 90*, 369–383.
14. Blondelle, S. E., and Lohner, K. (2000) Combinatorial libraries: a tool to design antimicrobial and antifungal peptide analogues having lytic specificities for structure-activity relationship studies. *Biopolymers 55*, 74–87.
15. Sajjan, U. S., Tran, L. T., Sole, N., Rovaldi, C., Akiyama, A., Friden, P. M., Forstner, J. F., and Rothstein, D. M. (2001) P-113D, an antimicrobial peptide active against Pseudomonas aeruginosa, retains activity in the presence of sputum from cystic fibrosis patients. *Antimicrob. Agents Chemother. 45*, 3437–3444.
16. Fernandez-Lopez, S., Kim, H. S., Choi, E. C., Delgado, M., Granja, J. R., Khasanov, A., Kraehenbuehl, K., Long, G., Weinberger, D. A., Wilcoxen, K. M., and Ghadiri, M. R. (2001) Antibacterial agents based on the cyclic D,L-alpha-peptide architecture. *Nature 412*, 452–455.
17. Hilpert, K., Volkmer-Engert, R., Walter, T., and Hancock, R. E. (2005) High-throughput generation of small antibacterial peptides with improved activity. *Nat. Biotechnol. 23*, 1008–1012.
18. Taboureau, O., Olsen, O. H., Nielsen, J. D., Raventos, D., Mygind, P. H., and Kristensen, H. H. (2006) Design of novispirin antimicrobial peptides by quantitative structure-activity relationship. *Chem. Biol. Drug Des. 68*, 48–57.
19. Hancock, R. E., and Sahl, H. G. (2006) Antimicrobial and host-defense peptides as new anti-infective therapeutic strategies. *Nat. Biotechnol. 24*, 1551–1557.
20. Marr, A. K., Gooderham, W. J., and Hancock, R. E. (2006) Antibacterial peptides for therapeutic use: obstacles and realistic outlook. *Curr. Opin. Pharmacol. 6*, 468–472.
21. Sonesson, A., Ringstad, L., Andersson Nordahl, E., Malmsten, M., Mörgelin, M., and Schmidtchen, A. (2006) Antifungal activity of C3a and C3a-derived peptides against Candida. *Biochim. Biophys. Acta 1768*, 346–353.
22. Nordahl, E. A., Rydengård, V., Nyberg, P., Nitsche, D. P., Mörgelin, M., Malmsten, M., Björck, L., and Schmidtchen, A. (2004) Activation of the complement system generates antibacterial peptides. *Proc. Natl. Acad. Sci. U.S.A. 101*, 16879–16884.
23. Alper, C. A. (1998) A history of complement genetics. *Exp. Clin. Immunogenet. 15*, 203–212.
24. Wessels, M. R., Butko, P., Ma, M., Warren, H. B., Lage, A. L., and Carroll, M. C. (1995) Studies of group B streptococcal infection in mice deficient in complement component C3 or C4 demonstrate an essential role for complement in both innate and acquired immunity. *Proc. Natl. Acad. Sci. U.S.A. 92*, 11490–11494.
25. Kerr, A. R., Paterson, G. K., Riboldi-Tunnicliffe, A., and Mitchell, T. J. (2005) Innate immune defense against pneumococcal pneumonia requires pulmonary complement component C3. *Infect. Immun. 73*, 4245–4252.
26. Pasupuleti, M., Walse, B., Nordahl, E. A., Mörgelin, M., Malmsten, M., and Schmidtchen, A. (2007) Preservation of antimicrobial properties of complement peptide C3a, from invertebrates to humans. *J. Biol. Chem. 282*, 2520–2528.
27. Richardson, J. S., and Richardson, D. C. (1988) Amino acid preferences for specific locations at the ends of alpha helices. *Science 240*, 1648–1652.
28. Lacroix, E., Viguera, A. R., and Serrano, L. (1998) Elucidating the folding problem of alpha-helices: local motifs, long-range electrostatics, ionic-strength dependence and prediction of NMR parameters. *J. Mol. Biol. 284*, 173–191.
29. Masny, A., and Plucienniczak, A. (2001) Fingerprinting of bacterial genomes by amplification of DNA fragments surrounding rare restriction sites. *BioTechniques 31*, 930–934, 936.
30. Lehrer, R. I., Rosenman, M., Harwig, S. S., Jackson, R., and Eisenhauer, P. (1991) Ultrasensitive assays for endogenous antimicrobial polypeptides. *J. Immunol. Methods 137*, 167–173.
31. Wiegand, I., Hilpert, K., and Hancock, R. E. (2008) Agar and broth dilution methods to determine the minimal inhibitory concentration (MIC) of antimicrobial substances. *Nat. Protoc. 3*, 163–175.

32. Turner, J., Cho, Y., Dinh, N. N., Waring, A. J., and Lehrer, R. I. (1998) Activities of LL-37, a cathelin-associated antimicrobial peptide of human neutrophils. *Antimicrob. Agents Chemother. 42*, 2206–2214.
33. Ringstad, L., Andersson Nordahl, E., Schmidtchen, A., and Malmsten, M. (2007) Composition Effect on Peptide Interaction with Lipids and Bacteria: Variants of C3a Peptide CNY21. *Biophys. J. 92*, 87–98.
34. Ringstad, L., Schmidtchen, A., and Malmsten, M. (2006) Effect of peptide length on the interaction between consensus peptides and DOPC/DOPA bilayers. *Langmuir 22*, 5042–5050.
35. Ringstad, L., Kacprzyk, L., Schmidtchen, A., and Malmsten, M. (2007) Effects of topology, length, and charge on the activity of a kininogen-derived peptide on lipid membranes and bacteria. *Biochim. Biophys. Acta 1768*, 715–727.
36. Greenfield, N., and Fasman, G. D. (1969) Computed circular dichroism spectra for the evaluation of protein conformation. *Biochemistry 8*, 4108–4116.
37. Sjogren, H., and Ulvenlund, S. (2005) Comparison of the helix-coil transition of a titrating polypeptide in aqueous solutions and at the air-water interface. *Biophys. Chem. 116*, 11–21.
38. Sandberg, M., Eriksson, L., Jonsson, J., Sjöstrom, M., and Wold, S. (1998) New chemical descriptors relevant for the design of biologically active peptides. A multivariate characterization of 87 amino acids. *J. Med. Chem. 41*, 2481–2491.
39. Huber, R., Scholze, H., Paques, E. P., and Deisenhofer, J. (1980) Crystal structure analysis and molecular model of human C3a anaphylatoxin. *Hoppe-Seyler's Z. Physiol. Chem. 361*, 1389–1399.
40. Hugli, T. E. (1990) Structure and function of C3a anaphylatoxin. *Curr. Top. Microbiol. Immunol. 153*, 181–208.
41. Lu, Z. X., Fok, K. F., Erickson, B. W., and Hugli, T. E. (1984) Conformational analysis of COOH-terminal segments of human C3a. Evidence of ordered conformation in an active 21-residue peptide. *J. Biol. Chem. 259*, 7367–7370.
42. Luo, P., and Baldwin, R. L. (2002) Origin of the different strengths of the (i,i+4) and (i,i+3) leucine pair interactions in helices. *Biophys. Chem. 96*, 103–108.
43. Maxwell, A. I., Morrison, G. M., and Dorin, J. R. (2003) Rapid sequence divergence in mammalian beta-defensins by adaptive evolution. *Mol. Immunol. 40*, 413–421.
44. Isaacson, R. E. (2003) MBI-226. Micrologix/Fujisawa. *Curr. Opin. Invest. Drugs 4*, 999–1003.
45. Sawai, M. V., Waring, A. J., Kearney, W. R., McCray, P. B., Jr., Forsyth, W. R., Lehrer, R. I., and Tack, B. F. (2002) Impact of single-residue mutations on the structure and function of ovispirin/novispirin antimicrobial peptides. *Protein Eng. 15*, 225–232.
46. Zavascki, A. P., Goldani, L. Z., Li, J., and Nation, R. L. (2007) Polymyxin B for the treatment of multidrug-resistant pathogens: a critical review. *J. Antimicrob. Chemother. 60*, 1206–1215.
47. Oren, Z., Ramesh, J., Avrahami, D., Suryaprakash, N., Shai, Y., and Jelinek, R. (2002) Structures and mode of membrane interaction of a short alpha helical lytic peptide and its diastereomer determined by NMR, FTIR, and fluorescence spectroscopy. *Eur. J. Biochem. 269*, 3869–3880.
48. Frecer, V., Ho, B., and Ding, J. L. (2004) De novo design of potent antimicrobial peptides. *Antimicrob. Agents Chemother. 48*, 3349–3357.
49. Hwang, P. M., and Vogel, H. J. (1998) Structure-function relationships of antimicrobial peptides. *Biochem. Cell Biol. 76*, 235–246.
50. Feder, R., Dagan, A., and Mor, A. (2000) Structure-activity relationship study of antimicrobial dermaseptin S4 showing the consequences of peptide oligomerization on selective cytotoxicity. *J. Biol. Chem. 275*, 4230–4238.
51. Nizet, V. (2007) Understanding how leading bacterial pathogens subvert innate immunity to reveal novel therapeutic targets. *J. Allergy Clin. Immunol. 120*, 13–22.
52. Foster, T. J. (2005) Immune evasion by staphylococci. *Nat. Rev. Microbiol. 3*, 948–958.
53. Peschel, A., and Sahl, H. G. (2006) The co-evolution of host cationic antimicrobial peptides and microbial resistance. *Nat. Rev. Microbiol. 4*, 529–536.
54. Harder, J., Bartels, J., Christophers, E., and Schröder, J. M. (2001) Isolation and characterization of human beta -defensin-3, a novel human inducible peptide antibiotic. *J. Biol. Chem. 276*, 5707–5713.
55. Glaser, R., Harder, J., Lange, H., Bartels, J., Christophers, E., and Schröder, J. M. (2005) Antimicrobial psoriasin (S100A7) protects human skin from Escherichia coli infection. *Nat. Immunol. 6*, 57–64.
56. Pitarch, A., Sanchez, M., Nombela, C., and Gil, C. (2002) Sequential fractionation and two-dimensional gel analysis unravels the complexity of the dimorphic fungus Candida albicans cell wall proteome. *Mol. Cell. Proteomics 1*, 967–982.
57. Henzler-Wildman, K. A., Martinez, G. V., Brown, M. F., and Ramamoorthy, A. (2004) Perturbation of the hydrophobic core of lipid bilayers by the human antimicrobial peptide LL-37. *Biochemistry 43*, 8459–8469.
58. Epand, R. F., Ramamoorthy, A., and Epand, R. M. (2006) Membrane lipid composition and the interaction of pardaxin: the role of cholesterol. *Protein Pept. Lett. 13*, 1–5.
59. Glukhov, E., Stark, M., Burrows, L. L., and Deber, C. M. (2005) Basis for selectivity of cationic antimicrobial peptides for bacterial versus mammalian membranes. *J. Biol. Chem. 280*, 33960–33967.
60. Sal-Man, N., Oren, Z., and Shai, Y. (2002) Preassembly of membrane-active peptides is an important factor in their selectivity toward target cells. *Biochemistry 41*, 11921–11930.
61. Jenssen, H., Lejon, T., Hilpert, K., Fjell, C. D., Cherkasov, A., and Hancock, R. E. (2007) Evaluating different descriptors for model design of antimicrobial peptides with enhanced activity toward P. aeruginosa. *Chem. Biol. Drug Des. 70*, 134–142.
62. Hilpert, K., Elliott, M. R., Volkmer-Engert, R., Henklein, P., Donini, O., Zhou, Q., Winkler, D. F., and Hancock, R. E. (2006) Sequence requirements and an optimization strategy for short antimicrobial peptides. *Chem. Biol. 13*, 1101–1107.
63. Bhonsle, J. B., Venugopal, D., Huddler, D. P., Magill, A. J., and Hicks, R. P. (2007) Application of 3D-QSAR for identification of descriptors defining bioactivity of antimicrobial peptides. *J. Med. Chem. 50*, 6545–6553.
64. Huang, H. W. (2000) Action of antimicrobial peptides: two-state model. *Biochemistry 39*, 8347–8352.

BI800991E